Neurobiology of Aging 76 (2019) 214.e11–214.e15

Contents lists available at ScienceDirect

Neurobiology of Aging

journal homepage: www.elsevier.com/locate/neuaging

Presence of tau astrogliopathy in frontotemporal dementia caused by a novel *Grn* nonsense (Trp2*) mutation

Estrella Gómez-Tortosa [a,*], Yalda Baradaran-Heravi [b,c], Valentina González Alvarez [d], María José Sainz [a], Cristina Prieto-Jurczynska [e], Rosa Guerrero-López [f], Pablo Agüero Rabes [a], Christine Van Broeckhoven [b,c], Julie van der Zee [b,c], Alberto Rábano Gutiérrez [d], on behalf of the EU EOD Consortium

[a] Department of Neurology, Fundación Jiménez Díaz, Madrid, Spain
[b] Neurodegenerative Brain Diseases group, Center for Molecular Neurology, VIB, Antwerp, Belgium
[c] Laboratory of Neurogenetics, Institute Born-Bunge, University of Antwerp, Antwerp, Belgium
[d] Brain Tissue Bank, Fundación CIEN, Instituto de Salud Carlos III, Madrid, Spain
[e] Department of Neurology, Hospital Infanta Elena, Madrid, Spain
[f] Instituto de Investigaciones Sanitarias Fundación Jiménez Díaz (IIS-FJD) and CIBERER Madrid, Spain

ARTICLE INFO

Article history:
Received 30 May 2018
Received in revised form 13 September 2018
Accepted 12 November 2018
Available online 20 November 2018

Keywords:
GRN mutations
Neuropathology
Tauopathy
ARTAG
Astrogliopathy

ABSTRACT

Frontotemporal lobar degeneration caused by *GRN* mutations is mainly associated with a TDP-43 type A proteinopathy. We present a family with autosomal dominant frontotemporal lobar degeneration caused by a novel *GRN* nonsense mutation (c.5G>A: p.Trp2*) in which the proband's brain also showed prominent glial tauopathy consistent with an aging-related tau astrogliopathy. Astrocytic tauopathy, 4R(+) and 3R(-) immunoreactive, was characterized by thorn-shaped astrocytes present in subpial, subependymal, and perivascular areas, and in gray matter; plus granular or fuzzy tau immunoreactivity in astrocytic processes in gray matter, either solitary or clustered in different regions. Some neurofibrillary tangles and pretangles, both 3R and 4R(+), were present in the medial temporal lobe but did not exhibit the characteristic distribution of Alzheimer's type pathology. This 4R-tau aging-related tau astrogliopathy is likely a co-occurring pathology, although an interaction between progranulin and tau proteins within the neurodegenerative process should not be ruled out.

1. Introduction

Frontotemporal lobar degeneration (FTLD) is currently subcategorized into three independent pathological phenotypes—tauopathies, TDP-43 proteinopathies, and FUS proteinopathies—each with consistent genetic correlations. Some cases with FTLD tauopathy have been found to carry *MAPT* mutations, whereas FTLD-TDP-43 proteinopathies have been associated with mutations in the *GRN* gene (subtype A), hexanucleotide expansion in *C9ORF72* (subtype B and A), or mutations in the *VCP* gene (subtype D) (Bang, 2015). So far, no known genetic correlations exist for either subtype C of TDP-43 proteinopathy or for FUS-related FTLD.

However, recent reports indicate that *GRN* mutations, which exert their effect through haploinsufficiency and reduced progranulin protein levels, can also be associated with certain tau pathology. Alzheimer's disease tangles and corticobasal degeneration features have been reported in *GRN* mutation carriers (Redaelli, 2018). In addition, Hosokawa (2017) have recently described a significant burden of tauopathy in the form of neuronal pretangles and glial inclusions in the brains of FTLD patients with *GRN* mutations.

We describe the clinical-pathological phenotype of a family with FTLD caused by a novel *GRN* nonsense mutation (c.5G>A: p.Trp2*) predicted to result in complete allele insufficiency. The proband showed neuropathology characterized by TDP-43 type A inclusions, but also extensive glial tauopathy consistent with an aging-related tau astrogliopathy (ARTAG) phenotype (Kovacs, 2016).

2. Methods

2.1. Family

This family belongs to a cohort of FTLD cases recruited from the memory clinic of Fundación Jiménez Díaz (Madrid, Spain). The

* Corresponding author at: Department of Neurology, Fundación Jiménez Díaz, Avenida de los Reyes Católicos 2, 28040 Madrid, Spain. Tel.: +34 91 5504800 ext. 2063; Fax: +34 91 5494764
E-mail address: egomezt@fjd.es (E. Gómez-Tortosa).

0197-4580/$ – see front matter © 2018 Elsevier Inc. All rights reserved.
https://doi.org/10.1016/j.neurobiolaging.2018.11.010

pattern of inheritance was autosomal dominant and two affected relatives, uncle and niece (II.3 and III.1, Fig. 1), had been examined. This study was approved by the Research Ethics Committee at Fundación Jiménez Díaz, and informed consent for genetic studies was provided by patients or their surrogates. The spouse of case II.3 consented to brain necropsy. Two asymptomatic, at-risk relatives have also been evaluated in the context of genetic counseling and presymptomatic testing.

2.2. Genetic study

Whole exome sequencing of the two affected plus one healthy relative (case II.2) was conducted by the EO EUD Consortium at the VIB-UAntwerp Center for Molecular Neurology (Antwerp, Belgium). Potential pathogenic variants were confirmed by Sanger sequencing (ABI 3730, Applied Biosystems). The segregation pattern was analyzed in the family.

2.3. Plasma progranulin levels

Plasma samples from five family members (two affected, a healthy relative, and two at-risk asymptomatic individuals) had been stored at −80°C. Progranulin levels were analyzed in the Laboratory of Neurology (Fundación Jiménez Díaz) by means of ELISA using a commercial kit (AdipoGen Inc, Seoul, South Korea) and following a standardized protocol. Our usual cutoff point to predict *GRN* mutations is <70 ng/mL.

2.4. Brain study

Neuropathological workup of case II.3 was performed at the Tissue Bank of the Fundación CIEN (Instituto de Salud Carlos III, Madrid, Spain). Five-micrometer–thick sections were cut from formalin-fixed and paraffin-embedded tissue obtained from multiple brain regions. Sections were stained with hematoxylin-eosin, Gallyas silver staining, and immunostained using monoclonal (mc) and polyclonal (pc) primary antibodies for beta-amyloid (mc, clone 6F/3D, DAKO), tau (including phospho-tau Ser202/Thr205, mc, clone AT8, and phospho-tau Thr212/Ser214, mc, clone AT100, both from Thermo Fisher Scientific; anti-tau 3-repeat isoform RD3, mc, clone 8E6/C11, and anti-tau 4-repeat (4R) isoform RD4, mc, clone 1E1/A6, both from Millipore), TDP-43 (pc, Proteintech; and mc, clone 2E2-D3, Abnova), alpha-synuclein (mc, clone KMS1, Leica Biosystems), ubiquitin (pc, Z0458, DAKO), and p62 (pc, Thermo Fisher Scientific). Presence of neuronal tau deposits (neurofibrillary tangles and pretangles) and different tau-immunoreactive astrocytic inclusions was recorded, along with their location (subpial, subependymal, perivascular, white matter, and gray matter). The pathologic profile of the glial tauopathy was defined in terms of the morphological type, location, and intensity of tau (+) cell inclusions, according to the criteria of Kovacs (2016).

3. Results

3.1. Clinical phenotypes

The two affected cases examined had manifested at a presenile age as behavioral (II.3) and nonfluent aphasia (III.1) variants of FTLD, respectively (Fig. 1). The first symptoms presented by case II.3 consisted of compulsive behaviors including hyperfagia, disinhibition, irritability, decreased verbal fluency, and ideomotor apraxia. CT scan and SPECT with HMPAO showed selective left temporal atrophy/hypoperfusion. Four years after onset, the patient had developed severe mixed aphasia and parkinsonism in right extremities. A CT scan obtained 1 year before his death showed severe frontotemporal (left predominant) atrophy (Fig. 1). Case III.1 began with apathy and decreased verbal fluency. After 2 years, she was aphasic and exhibited prominent dysexecutive syndrome. Currently—55 years of age—she is mute with right parkinsonian/corticobasal features, although no behavioral problems have developed. Her cerebral MRI scan and SPECT with HMPAO also reveal asymmetric frontotemporal (left and frontal predominant) neurodegeneration.

3.2. Whole exome sequencing

Analysis of the whole exome sequencing data was directed toward known neurodegenerative disease genes. This identified a *GRN* nonsense mutation, c.5G>A: p.Trp2* (confirmed by Sanger sequencing), carried by both patients and absent from the healthy elderly relative. This variant was absent from public control databases (dbSNP, ExAc, and the AD&FTD Mutation Database), and its predicted pathogenicity according to CADD score (Kircher, 2014) was 36 (>20 suggests pathogenicity). There were no *MAPT* mutations in the affected relatives, and screening for *C9ORF72* hexanucleotide expansion was also negative. All three relatives were heterozygous H1/H2 for the *MAPT* haplotype. One of the two at-risk relatives (III.3) turned out to be a carrier.

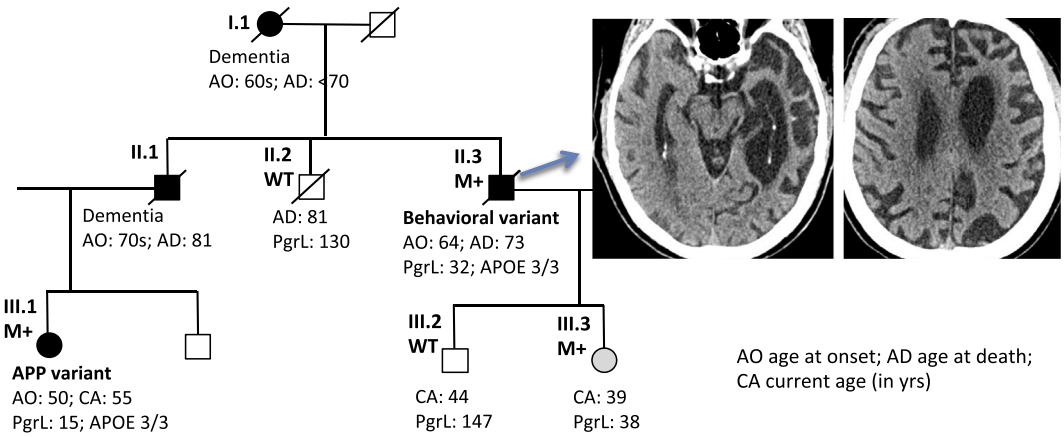

Fig. 1. Family tree including *GRN* Trp2* mutation status (M+ black: affected; M+ gray: asymptomatic carrier; WT: wild type), clinical phenotypes, and progranulin plasma levels (PgrL in ng/mL). CT scan images of the proband (II.3) 1 year before his death.

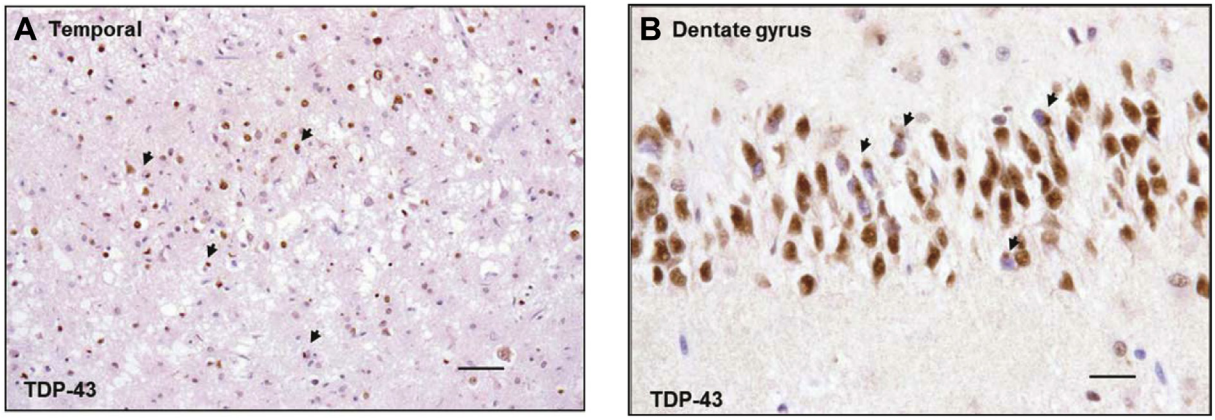

Fig. 2. TDP-43 immunoreactive inclusions in the cerebral cortex, mainly in layer 2, consistent with TDP-43 type A proteinopathy (A). TDP-43 immunoreactive inclusions were also present in dentate gyrus (B).

3.3. Plasma progranulin levels

Pathogenicity of the *GRN* mutation was further supported by reduced plasma progranulin levels in the two affected patients and the asymptomatic carrier (all below 40 ng/mL, see values in Fig. 1), compared with levels in the two noncarrier relatives (≥130 ng/mL).

3.4. Neuropathology (case II.3)

Macroscopic evaluation showed severe bilateral frontotemporal and inferior parietal atrophy (left predominant) with an unfixed brain weight of 1053 g. On hematoxylin-eosin staining, near complete neuronal loss with neuropil spongiosis was observed in the orbitofrontal, temporal, and insular cortices. Entorhinal cortex and amygdala showed severe neuronal loss and gliosis. Hippocampal sclerosis was observed including subiculum and CA1-2, with relative sparing of dentate gyrus.

Beta-amyloid was found in very scattered diffuse plaques present in CERAD cortical areas. There was no amyloid angiopathy. α-Synuclein immunostaining was negative all throughout the brainstem and cortex.

TDP-43 immunoreactivity (Fig. 2) was present in cortex and characterized by short dystrophic neurites and neuronal cytoplasmic inclusions concentrated primarily in layer 2, consistent

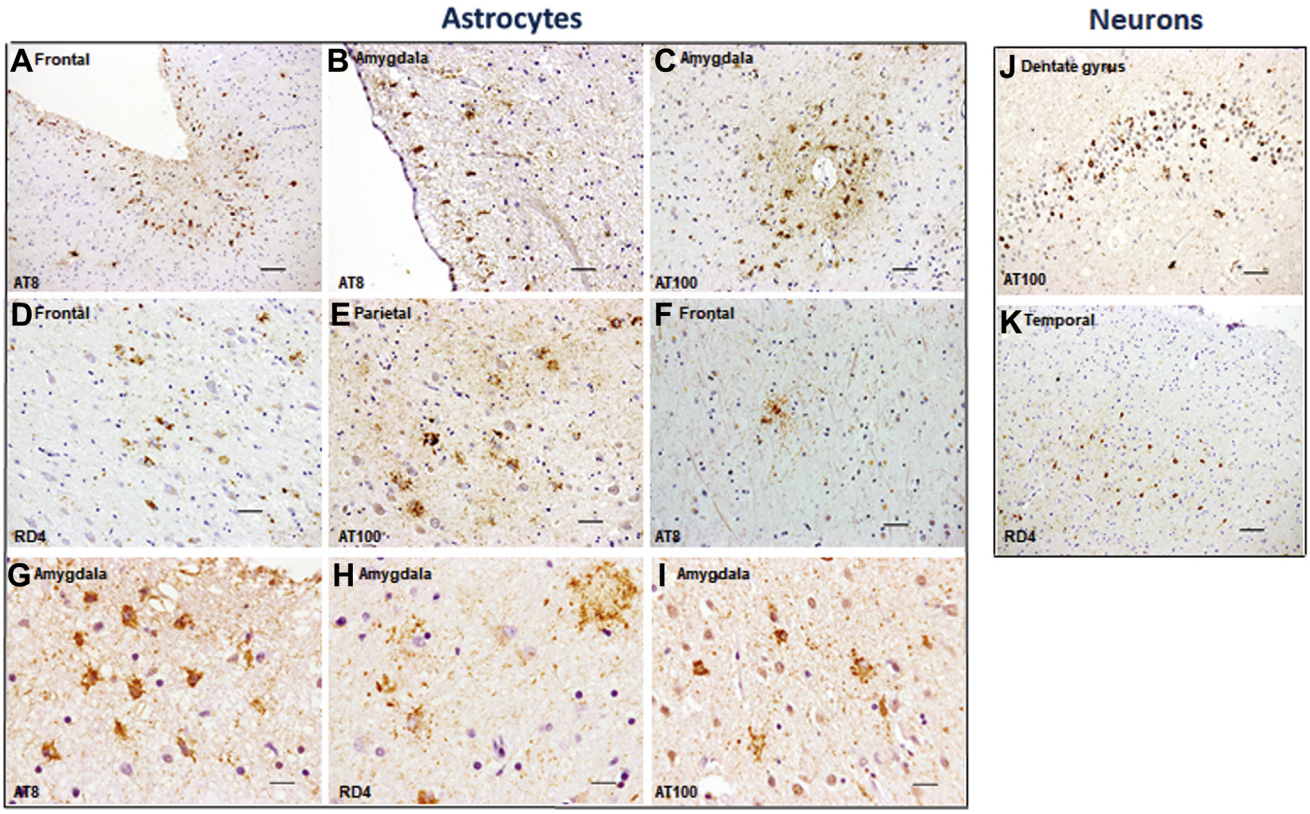

Fig. 3. Tau immunoreactive inclusions: different ARTAG types were found in different locations: subpial (A), subependymal (B), perivascular (C), gray matter (D, E), and white matter (F) locations. TSA and GFA were detected by AT8 (G), AT100 (I), and 4R-tau (H) antibodies, and were negative for the 3R isoform antibody. Neuronal inclusions (G, H) were identified in the medial temporal lobe, showing immunoreactivity for both 3R and 4R tau antibodies. Scale bar: 150 μm (50 in G–I) . Bottom left: antibody used.

with type A TDP-43 proteinopathy (Mackenzie, 2011). There were also TDP-43 immunoreactive neurons in dentate gyrus, in the hippocampal sclerosis segment, and a few in the striatum and nucleus basalis of Meynert. No intranuclear TDP-43 immunoreactive inclusions were observed. No tau-negative, p62-immunoreactive inclusions were observed in any cortical or subcortical regions.

Tau accumulation was characterized by abundant phospho-tau (+) inclusions; these were predominantly astrocytic and, less frequently, neuronal tau deposits. Thorn-shaped astrocytes (TSA) and granular or fuzzy tau immunoreactivity in processes of astrocytes (GFA)—the two major cytomorphologies of the recently characterized ARTAG phenotype (Kovacs, 2016)—were detected by AT8 and AT100 and a 4R tau antibody, and were negative for the 3R isoform antibody. TSA were clearly Gallyas-positive, whereas GFA showed inconsistent slightly stained granular deposits in the perikaryon. The neuropil contained a moderate number of slender positive threads. Different ARTAG types, according to the brain region involved, were found (Fig. 3): subpial (A), subependymal (B), perivascular (C), gray matter (D, E), and white matter (F) locations. No inclusions characteristic of other primary tauopathies were found. The Table summarizes the regional distribution and intensity of involvement by astroglial and neuronal tau pathology following the Kovacs (2016) evaluation strategy for ARTAG. TSA and GFA coexisted in multiple regions, with a high presence found in the anterior medial temporal lobe. TSA were observed mainly in subpial localization, the deep segments of gyri, and in subependicular and perivascular areas, both in the gray and white matter, whereas GFA were present either in the white matter or clustered in different gray matter regions of the brain. Neuronal tau pathology was detected as pretangles and NFTs in different brain regions, with a higher presence in the medial temporal lobe, not exhibiting a characteristic distribution for Alzheimer's type pathology. These neuronal inclusions were immunoreactive for both 3R and 4R tau antibodies Table 1.

4. Discussion

The presence of this ARTAG phenotype in the brain of a patient with TDP-43 type A FTLD pathology associated with a *GRN* nonsense mutation suggests two possible scenarios: the co-occurrence of two independent processes, or a relationship underlying both pathologies.

The first scenario, concomitance or co-occurrence of two neuropathologies, appears the most likely in light of recent reports showing the high prevalence of concomitant proteinopathies in brains of cases with neurodegenerative diseases, which increases with the age at death (Robinson, 2018). In particular, accumulation of neuronal tau as neurofibrillary tangles seems to be almost

Table 1
Regional distribution and intensity of involvement (color gradient) by astroglial and neuronal tau pathology, according to the evaluation strategy of Kovacs et al. for ARTAG

	Step 1	step 2	Step 3					
ASTROCYTES	Type	Major anatomical	Severity in detailed regional distribution and extent of ARTAG					
	Subpial	MTL	Inf. Temporal Gy	Hippocampus	Entorhinal cortex	Amydala		
		Lobar	Frontal	Cingular cortex	Insular cortex	Parietal	Occipital	Temporal
		Subcortical				basal forebrain	Hypothalamus	
		Brainstem	Mesencephalon			Pons	medulla Obl.	
	Subpendymal	MTL	Temporal horn			Amygdala		
		Lobar	LV: Frontal horn				LV: Occipital horn	
		Subcortical	LV: Caudate	3V: Thalamus				Hypothalamus
		Brainstem	Aq/Mesencephalon	Aq/Pons	Aq/Medulla obl.			
	perivascular	MTL	Inf. Temporal Gy	Hippocampus	Entorhinal cortex	Amygdala		
		Lobar	Frontal	Cingular cortex	Insular cortex	Parietal	Occipital	Temporal
		Subcortical	Accumbens	Caud/Put	Globus pallidus	basal forebrain	Hypothalamus	
		Brainstem	Mesencephalon			Pons	Medulla obl.	
	White matter	MTL	Inf. Temporal Gy	Hippocampus	Entorhinal cortex	Amygdala		
		Lobar	Frontal	Cingular cortex	Insular cortex	Parietal	Occipital	Temporal
		Subcortical	Internal capsule			Subinsular	Pencil fibers	
		Brainstem	Cerebral pedunculi			Pyramids	Midline	
	Gray matter	MTL	Inf. Temporal Gy	Hippocampus	Entorhinal cortex	Amygdala		
		Lobar	Frontal	Cingular cortex	Insular cortex	Parietal	Occipital	Temporal
		Subcortical	Accumbens	Caud/Put	Globus pallidus	basal forebrain	Hypothalamus	
		Brainstem	Substantia nigra			Pons	Medulla obl.	
NEURONS	Gray matter	MTL	Inf. Temporal Gy	Hippocampus	Entorhinal cortex	Amygdala		
		Lobar	Frontal	Cingular cortex	Insular cortex	Parietal	Occipital	Temporal
		Subcortical	Accumbens	Caud/Put	Globus pallidus	basal forebrain	Hypothalamus	
		Brainstem	Substantia nigra			Pons	Medulla obl.	

TSA and GFA coexisted in multiple regions, with a higher presence in the anterior medial temporal lobe (MTL). Neuronal tau pathology was detected as pretangles and NFTs in different brain regions, with higher presence in the MTL.
Key: ARTAG, aging-related tau astrogliopathy; TSA, thorn-shaped astrocytes; GFA, granular or fuzzy tau immunoreactivity in astrocytic processes.

universal in brains with all other primary neurodegenerative pathologies (Robinson, 2018). Recent studies suggest that in cases with pathologically confirmed FTLD, multiple neuronal pathologies appear with equal prevalence in young and elderly cases (Tan and Halliday, 2017). Furthermore, previous case reports describe concomitant tau pathology in *GRN* mutation carriers (Hosokawa, 2017; Leverenz, 2007) and suggest that *GRN* insufficiency could be associated with multiple proteinopathies, including TDP-43, tau, and alpha-synuclein deposition.

Most of these studies concentrate on the co-occurrence of neuronal inclusions and have paid less attention to the presence of glial pathology. However, the report by Hosokawa (2017) is highly relevant to our description because the authors examine free-floating sections of four cases with three different *GRN* mutations and find tau immunoreactivity in astrocytes in all of them (massive in one). In particular, the massive astrogliopathy described in that case resembles our studied brain in terms of regional distribution and staining characteristics, although the astrocyte morphology is reported as "bush-like" rather than "thorn-shaped". Hosokawa (2017) further studied paraffin-embedded sections of another nine cases with *GRN* mutations and found some AT8 immunoreactivity in the majority, but to a lesser extent. The authors emphasize that the sensitivity to detect tau deposition is higher in free-floating tissue compared with paraffin-embedded sections.

A second scenario could be that the presence of ARTAG would be related to the *GRN* mutation condition and progranulin insufficiency. Some research studies support that progranulin reduction may contribute to abnormal tau deposition. An SNP *GRN* variant (rs5848) has been associated with the risk of Alzheimer's disease (Lee, 2011) and correlates with increased CSF tau levels (Takahashi, 2017). In animal models, a reduction in progranulin in tau transgenic mice (P301L tau/*GRN*-deficient mouse model) is associated with increased tau accumulation (Hosokawa, 2015).

The mechanisms by which *GRN* insufficiency may be able to contribute to tauopathy could be speculated in terms of the complex roles of progranulin in the brain. Progranulin is a pleiotropic glycoprotein with growth factor–like properties and neuronal effects including regulation of neurite outgrowth, synapse biology, stress response, and lysosomal functions (Petkau and Leavitt, 2014). *GRN*-deficient mouse models show an aging pathological phenotype characterized by increased astrocytic and microglial proliferation and highly accelerated deposition of lipofuscin (Petkau et al, 2016; Yin, 2010). Progranulin contributes to long-term cell survival and decreasing *GRN* expression likely impairs cell resistance to aging and other degenerative diseases. Particularly, GRN-deficient hippocampal cells in vitro are more vulnerable to direct cytotoxicity of macrophages and microglia as well as to deprivation of oxygen and glucose (Yin, 2010). It is possible that a tau astrogliopathy develops because astrocytes are more vulnerable than neurons, as has been shown in preclinical corticobasal degeneration cases, where a tau astrogliopathy seems to be a prodromal stage before the advance of extensive neuronal tauopathy (Ling, 2016). Furthermore, it has been suggested that some ARTAG features (GFA) can be premature stages of the astrocytic inclusions characterizing the primary aging-related tauopathies (Kovacs, 2017; Kovacs, 2018).

Finally, the contribution of the glial tauopathy to the clinical phenotype has yet to be defined. Some clinicopathological studies suggest that circumscribed ARTAG may present clinically with focal symptoms such as aphasia (Munoz, 2007), whereas in cases with widespread pathology, dementia with or without parkinsonism might be the clinical presentation (Kovacs, 2013).

In conclusion, this family adds support to the notion that genetic variations in *GRN* are associated with a variety of neurodegenerative proteinopathies including astroglial tauopathy.

Disclosure

The authors have no financial disclosures to report.

Acknowledgments

This work was supported by grants from the Ministry of Sciences and Technology, (SAF2010-18277), Instituto de Investigación Carlos III (FIS14/00,099), and FEDER funds, Spain. CVB, JvdZ and YBH were in part funded by the Flemish Government initiated Impulse Program on Networks for Dementia Research (VIND) and the Methusalem Excellence Program; the Research Foundation Flanders (FWO) and the University of Antwerp Research Fund.

The authors thank the family members who have collaborated in this study; G. Sánchez for the collection and processing of blood samples; I. Rodal for neuropathological techniques; and O. Shaw for editing the article.

References

Bang, J., 2015. Non-Alzheimer's dementia 1. Frontotemporal dementia. Lancet 386, 1672–1682.
Hosokawa, M., 2015. Progranulin reduction is associated with increased tau phosphorylation in P301L tau transgenic mice. J. Neuropath Exp. Neurol. 74, 158–165.
Hosokawa, M., 2017. Accumulation of multiple neurodegenerative disease-related proteins in familial frontotemporal lobar degeneration associated with granulin mutation. Sci. Rep. 7, 1513.
Kircher, M., 2014. A general framework for estimating the relative pathogenicity of human genetic variants. Nat. Genet. 46, 310–315.
Kovacs, G.G., 2013. Non-Alzheimer neurodegenerative pathologies and their combinations are more frequent than commonly believed in the elderly brain: a community-based autopsy series. Acta Neuropathol. 126, 365–384.
Kovacs, G.G., 2016. Aging-related tau astrogliopathy (ARTAG): harmonized evaluation strategy. Acta Neuropathol. 131, 87–102.
Kovacs, G.G., 2017. Evaluating the patterns of aging-related tau astrogliopathy unravels novel insights into brain aging and neurodegenerative diseases. J. Neuropathol. Exp. Neurol. 76, 270–288.
Kovacs, G.G., 2018. Sequential stages and distribution patterns of aging-related tau astrogliopathy (ARTAG) in the human brain. Acta Neuropathol. Commun. 6, 50.
Lee, M.J., 2011. rs5848 variant of progranulin gene is a risk of Alzheimer's disease in the Taiwanese population. Neurodegener. Dis. 8, 216–220.
Leverenz, J.B., 2007. A novel progranulin mutation associated with variable clinical presentation and tau, TDP43 and alpha-synuclein pathology. Brain 130, 1360–1374.
Ling, H., 2016. Astrogliopathy predominates the earliest stage of corticobasal degeneration pathology. Brain 139, 3237–3252.
Mackenzie, I.R.A., 2011. A harmonized classification system for FTLD-TDP pathology. Acta Neuropathol. 122, 111–113.
Munoz, D.G., 2007. Argyrophilic thorny astrocyte clusters in association with Alzheimer's disease pathology in possible primary progressive aphasia. Acta Neuropathol. 114, 347–357.
Petkau, T.L., Leavitt, B.R., 2014. Progranulin in neurodegenerative disease. Trends Neurosci. 37, 388–398.
Petkau, T.L., Hill, A., Leavitt, B.R., 2016. Core neuropathological abnormalities in progranulin-deficient mice are penetrant on multiple genetic backgrounds. Neuroscience 315, 175–195.
Redaelli, V., 2018. Alzheimer neuropathology without frontotemporal lobar degeneration hallmarks (TAR DNA-binding protein 43 inclusions) in missense progranulin mutation Cys139Arg. Brain Pathol. 28, 72–76.
Robinson, J.L., 2018. Neurodegenerative disease concomitant proteinopathies are prevalent, age-related and APOE4-associated. Brain 141, 2181–2193.
Takahashi, H., 2017. Opposing effects of progranulin deficiency on amyloid and tau pathologies via microglial TYROBP network. Acta Neuropathol. 133, 785–807.
Tan, R.H., Yang, Y., Halliday, G.M., 2017. Multiple neuronal pathologies are common in young patients with pathologically proven Frontotemporal lobar degeneration. Neuropathol. Appl. Neurobiol. https://doi.org/10.1111/nan.12455. In Press.
Yin, F., 2010. Exaggerated inflammation, impaired host defense, and neuropathology in progranulin-deficient mice. J. Exp. Med. 207, 117–128.